

Received October 9, 2021, accepted October 22, 2021, date of publication November 2, 2021, date of current version November 9, 2021.

Digital Object Identifier 10.1109/ACCESS.2021.3125097

MIMO Antenna System With Pattern Diversity for Sub-6 GHz Mobile Phone Applications

UZAIR AHMAD¹, SADIQ ULLAH¹, (Senior Member, IEEE),
UMAIR RAFIQUE², (Student Member, IEEE), DONG-YOU CHOI³,
RIZWAN ULLAH¹, BABAR KAMAL⁴, AND ASHFAQ AHMAD³

¹Telecommunication Engineering Department, University of Engineering & Technology, Mardan, Khyber Pakhtunkhwa 23200, Pakistan

²Department of Information Engineering, Electronics and Telecommunications, Sapienza Università di Roma, 00184 Rome, Italy

³Communication and Wave Propagation Laboratory, Department of Information and Communication Engineering, Chosun University, Gwangju 61452, South Korea

⁴Center of Intelligent Acoustics and Immersive Communications, Northwestern Polytechnical University, Xi'an 710072, China

Corresponding author: Dong-You Choi (dychoi@chosun.ac.kr)

ABSTRACT A MIMO antenna system is designed and presented for sub-6 GHz mobile phone applications. The proposed antenna design consists of six loop-type radiation elements. From the six elements, four elements are placed at the corners of the mobile phone PCB by following pattern diversity configuration, while the rest of the two elements are placed in the center of the PCB. Furthermore, a 50Ω coaxial connector is utilized to feed the antenna elements. From the presented results, it is demonstrated that the elements placed at the edges are resonating at 2.5 GHz, and the center placed elements provide resonance at 3.5 GHz. Moreover, according to $S_{11} \leq -6$ dB, the impedance bandwidth for both the bands is 790 MHz (2.3-3.09 GHz) and 1.18 GHz (2.99-4.17 GHz), respectively; while for $S_{11} \leq -10$ dB, the impedance bandwidth for both the bands is noted to be 340 MHz (2.38-2.72 GHz) and 650 MHz (3.17-3.84 GHz), respectively. A gain of more than 4 dBi and >85% radiation efficiency are achieved for the single radiation element. The presented antenna design also provides sufficient radiation coverage supporting different sides of the mobile phone PCB. In addition, the effects of the human hand and head on antenna's performance are studied and it was observed that the proposed antenna system provides acceptable properties in the data mode and talk mode.

INDEX TERMS 5G technology, loop-type elements, MIMO, mobile phone, pattern diversity.

I. INTRODUCTION

With the development in fifth-generation (5G) mobile communication systems, many research societies are focusing to achieve high data rate at low-cost [1], [2]. This demand can be fulfilled by utilizing multiple-input multiple-output (MIMO) technology because it is the key to realize a high data rate [3]. Furthermore, one of the keys to improving the channel capacity of MIMO systems is to design multiple antennas for independent channels [4], [5]. For 5G mobile communication systems, a large number of antenna elements need to be designed to fulfill the requirements of high data rate [6]. In addition, the designed antenna should be low-profile, small in size so that it can easily be integrated into hand-held devices, such as mobile phones. Moreover, the MIMO antennas should provide low mutual coupling, which

is the stringent requirement of a 5G mobile communication system [4], [5]. Recently, several kinds of MIMO smartphone antennas have been designed and presented for sub-6 GHz mobile terminals. The reported antenna designs are either non-planar, occupies a large area on a smartphone mainboard, and consists of complex structures.

In [7]–[15], non-planar MIMO antenna systems were proposed for sub-6 GHz mobile phone applications. Since the configuration of the designed antennas is non-planar; therefore, their implementation is critical and they cannot easily be integrated into hand-held devices. To overcome this limitation, planar antennas are being used because they are low-profile, their fabrication is simple, and they have the capability of easy integration into smartphones. Like in [16], [17], a ten and eight elements L-shaped slot-coupled planar MIMO antenna systems were designed for dual-band sub-6 GHz smartphone applications. In [18]–[21], the authors designed dual-polarized MIMO

The associate editor coordinating the review of this manuscript and approving it for publication was Pavlos I. Lazaridis.

TABLE 1. Comparison among proposed and earlier reported MIMO antennas for sub-6 GHz 5G applications.

| Ref. | Board Size (mm ²) | No. of Elements | Frequency Band (GHz) | Efficiency (%) | Isolation (dB) | ECC |
|----------------------------|-------------------------------|-----------------|-------------------------|----------------|----------------|---------|
| Non-planar Antennas | | | | | | |
| [7] | 150×75 | 8 | 3.4-3.6 | 70 | >15 | <0.0125 |
| [8] | 150×73 | 8 | 3.4-3.6 | 61 | >17 | <0.07 |
| [9] | 150×75 | 8 | 2.5-3.6 | 65 | >13 | <0.02 |
| [10] | 150×73 | 4 | 3.4-3.6 | 30-50 | >17 | <0.1 |
| [11] | 124×74 | 8 | 3.3-3.6 | 40 | >15 | <0.15 |
| [12] | 150×75 | 8 | 3.3-6 | >40 | >10 | <0.12 |
| [13] | 150×75 | 8 | 3.4-3.6 | 50-60 | >13 | <0.08 |
| [14] | 150×75 | 8 | 3.25-3.82/4.79-6.2 | 60-70 | >10.5 | <0.12 |
| [15] | 110×55 | 2 | 3.5/4.3 | 90 | 21 | <0.05 |
| Planar Antennas | | | | | | |
| [16] | 150×80 | 10 | 3.5/5.5 | 65/80 | >15 | <0.15 |
| [17] | 150×80 | 8 | 3.4-3.6 | >62 | >17 | <0.05 |
| [18] | 150×75 | 8 | 3.2-4 | 80 | 20 | <0.01 |
| [19] | 150×75 | 8 | 3.4-4.4 | >90 | >16 | <0.005 |
| [20] | 150×75 | 8 | 2.46-2.65/3.4-3.7/5.6-6 | >60 | >10 | <0.01 |
| [21] | 150×75 | 8 | 3.3-3.9 | 60-80 | 18 | <0.005 |
| [22] | 150×80 | 8 | 3.4-3.6 | 60-70 | >10 | <0.1 |
| [23] | 130×70 | 8 | 3.4-3.6 | 70-80 | >10 | <0.1 |
| This Work | 150×75 | 6 | 2.38-2.72/3.19-3.84 | 86-92 | >15 | <0.17 |

[7], [10] did not define the method to calculate ECC.

[15], [18]–[23] calculated ECC using S-parameters.

antennas for 5G cellular applications. The presented designs provide a dual-polarization and wideband response, but they suffered due to high mutual coupling. In [22], [23], the authors designed ten and nine-port MIMO antenna systems for 2G/3G/4G and sub-6 GHz mobile phone applications. The presented design configurations were the same as presented in [16], [17]. The presented MIMO antennas were low-profile and simple in nature, but they occupy a large area on the printed circuit board (PCB). Some researchers also designed reconfigurable [24] and low pass filter (LPF) [25] based planar antenna for both sub-6 GHz and millimeter-wave (mm-wave) applications, but their structures are complex in nature.

In this paper, a six-element MIMO antenna system is designed and presented for future 5G-enabled smartphone applications. A loop-type element fed through a 50Ω coaxial connector is selected for a single antenna design. To provide space for other smartphone components, four elements resonating at 2.5 GHz are placed at the corners of the mainboard, which follows the principle of pattern diversity configuration, while two elements, meant for 3.5 GHz frequency band, are placed in the center of the board. The designed MIMO configuration offers low mutual coupling between antenna elements, which tends to achieve a low envelope correlation coefficient (ECC), high total active reflection coefficient (TARC), and high diversity gain (DG). For the verification of

the suitability of the proposed MIMO system, a comparison between previously reported and proposed MIMO antennas is provided in Table 1.

II. PROPOSED MIMO ANTENNA SYSTEM

The design of the proposed MIMO antenna system is shown in Fig. 1. The radiation elements are printed on a conductor-backed low-cost 0.8mm thick FR-4 substrate having relative permittivity (ϵ_r) 4.4 and loss tangent ($\tan \delta$) 0.025. For less area consumption on the PCB, loop-type structures are selected for antenna design. From Fig. 1, one can observe that the designed antenna system consists of six loop-type radiation elements placed at the corners and the center of PCB having dimensions $W_s \times L_s$. The antenna elements (Ant-1 to Ant-4) placed at the corners of the PCB are meant for 2.5 GHz frequency band, while the antenna elements (Ant-5 and Ant-6) placed in the center are designed to get resonance at 3.5 GHz. The space along L_s is left empty for the integration of 2G/3G/4G antennas and millimeter-wave (mm-wave) arrays. The resonant length of each antenna element is equal to one guided wavelength (λ_g) at 2.5 GHz and 3.5 GHz, and it can be calculated as:

$$\lambda_g = \frac{c}{f_r \sqrt{\epsilon_{\text{reff}}}} = \frac{\lambda_0}{\sqrt{\epsilon_{\text{reff}}}} \quad (1)$$

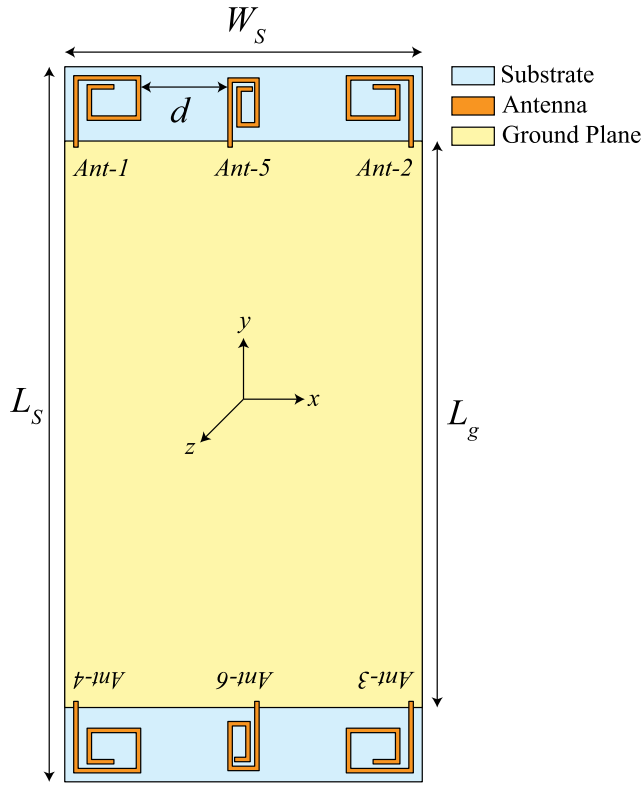


FIGURE 1. Layout of the proposed MIMO antenna.

where

$$\epsilon_{\text{reff}} = \frac{\epsilon_r + 1}{2} \quad (2)$$

In the above-mentioned equations, c represents the speed of light having value $3 \times 10^8 \text{ms}^{-1}$, f_r is the resonant frequency in GHz, λ_0 stands for free-space wavelength, and ϵ_{reff} denotes effective relative permittivity of the dielectric substrate.

By using (1), the resonant length of the antenna elements for 2.5 GHz and 3.5 GHz are noted to be 73mm and 52mm, respectively; while the optimized values are 67mm and 46mm, respectively. Moreover, the line width of each antenna element is chosen to be 1mm. It is also worth mentioning that the maximum occupied area by the single antenna element is $15 \times 16 \text{mm}^2$. The detailed design parameters of antenna elements are illustrated in Fig. 2(a) and (b), and their optimized values are listed in Table 2.

The proposed MIMO antenna system has been designed and simulated in CST Microwave Studio, and its respective

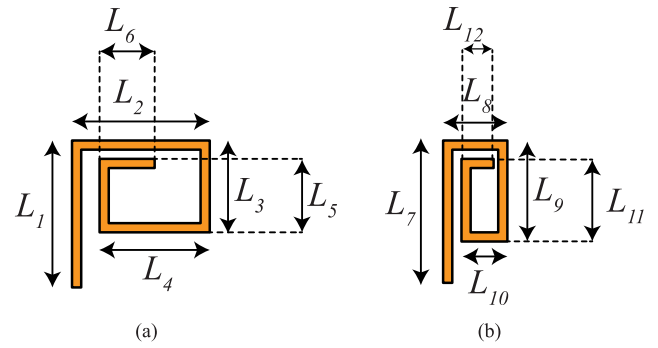


FIGURE 2. Schematic of the proposed antenna elements for (a) Ant-1 to Ant-4 (b) Ant-5 and Ant-6.

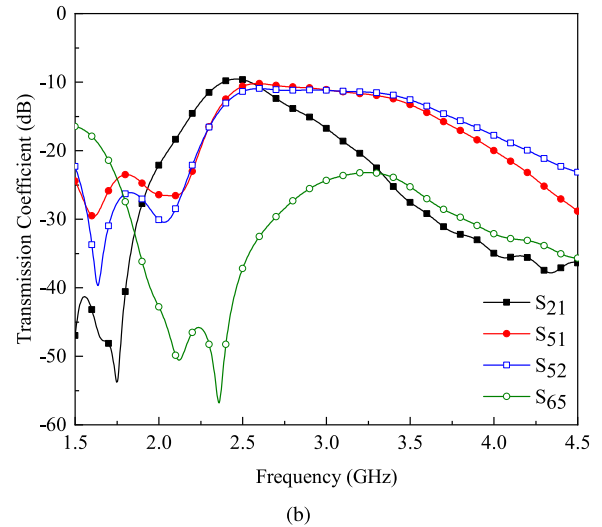
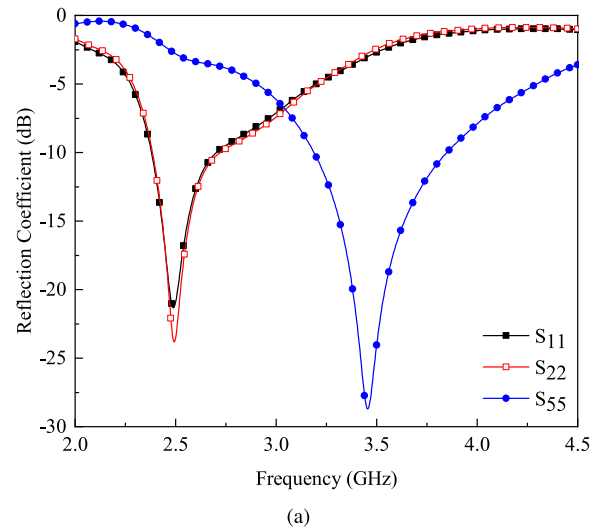


FIGURE 3. Simulated (a) reflection and (b) transmission coefficient of the proposed MIMO antenna.

TABLE 2. Design parameters of the proposed MIMO antenna (all dimensions in mm).

| L_S | W_S | L_g | d | L_1 | L_2 | L_3 | L_4 |
|-------|-------|-------|-------|-------|----------|----------|----------|
| 150 | 75 | 118 | 17.5 | 16 | 15 | 10 | 12 |
| L_5 | L_6 | L_7 | L_8 | L_9 | L_{10} | L_{11} | L_{12} |
| 8 | 6 | 15.5 | 6 | 10 | 4 | 8 | 2.5 |

reflection and transmission coefficient results are shown in Fig. 3. Due to the symmetrical properties between the antenna elements, the reflection and transmission coefficient results of Ant-1, Ant-2, and Ant-5 are presented. From Fig. 3(a),

it has been observed that the antenna elements are resonating well for the desired frequency bands, i.e. 2.5 GHz and 3.5 GHz. The -6 dB impedance bandwidth for 2.5 GHz and 3.5 GHz frequency band is noted to be 790 MHz (2.3-3.09 GHz) and 1.18 GHz (2.99-4.17 GHz), respectively; while -10 dB impedance bandwidth for both the bands is noted to be 340 MHz (2.38-2.72 GHz) and 650 MHz (3.19-3.84 GHz), respectively. Furthermore, from Fig. 3(b), it can be noted that the minimum isolation between Ant-1, Ant-2, and Ant-5 is equal to 10 dB, while the minimum noted isolation is 25 dB between Ant-5 and Ant-6.

To validate the isolation mechanism between array elements, the surface current distribution of the proposed MIMO array is plotted in Fig. 4. The plot of Fig. 4 is extracted by exciting one port at a time. In this case, port-1, port-2, and port-5 are excited one by one. It can be observed from the figure that the current is uniformly distributed on the excited port, and it has a negligible effect on adjacent antenna elements. These results also validate the high performance of the proposed MIMO array.

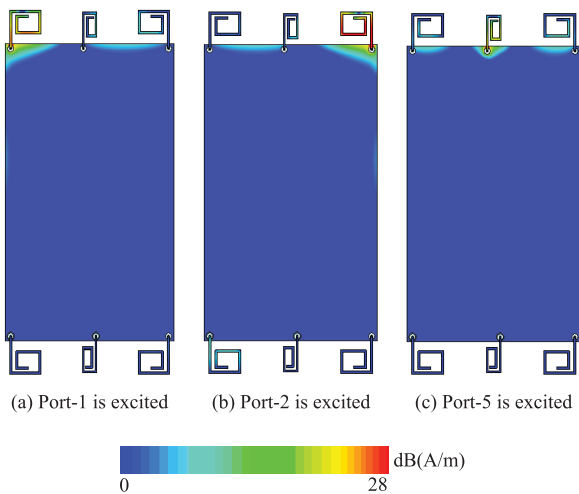


FIGURE 4. Surface current distribution of the proposed MIMO antenna at (a) port-1, (b) port-2 and (c) port-5.

The simulated three-dimensional (3-D) radiation patterns of the proposed MIMO antenna are shown in Fig. 5. As can be observed from the figure, the proposed MIMO antenna generates different vertical and horizontal polarized radiation patterns for both frequency bands. The generated radiation patterns validate that the designed MIMO antenna can provide pattern diversity, which is a useful characteristic for future smartphone applications. Furthermore, the gain of the proposed MIMO array fluctuates in the range of 4-6 dBi.

III. FABRICATION AND MEASUREMENTS

For the validation of simulated data, the proposed MIMO antenna system is fabricated and measured. The front and backside of the fabricated prototype are shown in Fig. 6. For measurement purposes, a flange-mounted coaxial connector with 50Ω characteristics impedance is used. Furthermore, the

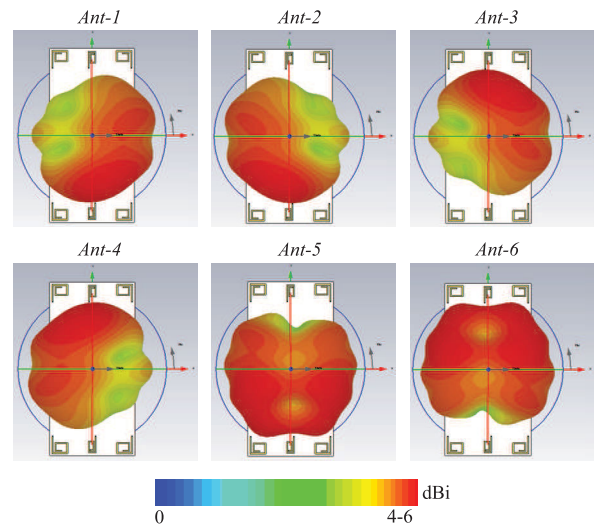


FIGURE 5. 3-D radiation patterns for designed MIMO antenna.

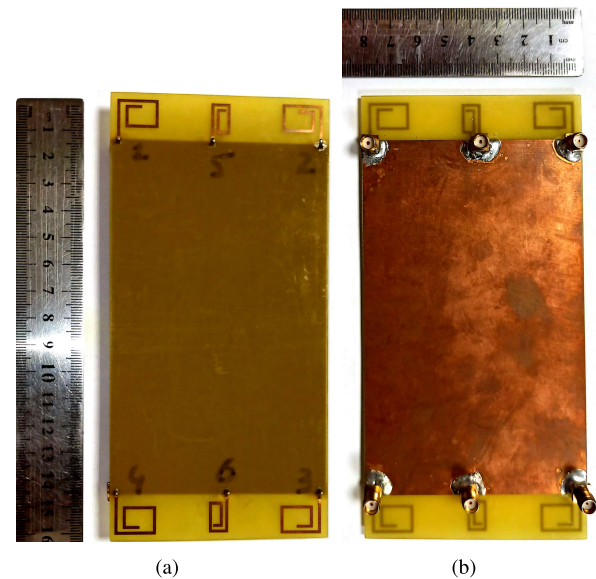


FIGURE 6. Fabricated prototype of the proposed MIMO antenna (a) front side (b) back side.

S-parameters of the proposed antenna are measured using Agilent Technologies Vector Network Analyzer N5232A.

Figure 7 illustrates the comparison between simulated and measured reflection and transmission coefficient results of the proposed MIMO antenna. From the figure, it can be observed that the measurement results are well in agreement with the simulated data. A slight mismatch has been observed between both reflection coefficient results, which arise due to imperfect SMA connector soldering and fabrication tolerances. Furthermore, it has been observed from Fig. 7 that the measured isolation between the antenna elements is much better compared to the simulated one. The measured isolation between Ant-1 and Ant-2 is noted to be 15 dB, while it is equal to ≈ 18 dB between Ant-1, Ant-2, and Ant-5.

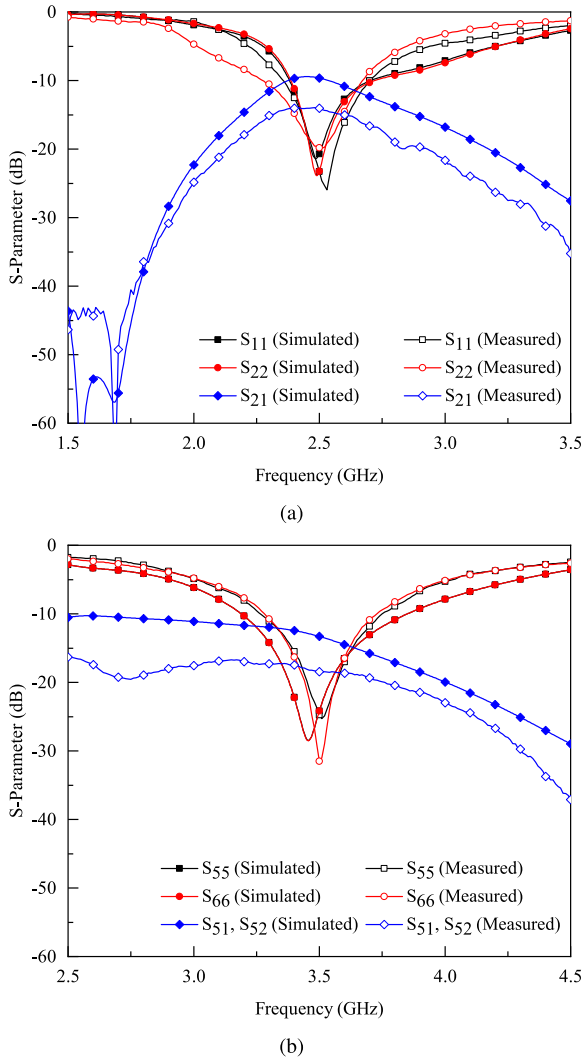


FIGURE 7. Simulated and measured reflection and transmission coefficient results of the proposed MIMO antenna for (a) 2.5 GHz and (b) 3.5 GHz frequency bands.

For far-field measurements, the proposed MIMO antenna is tested in an anechoic chamber using a standard procedure. A horn antenna is used as a reference antenna, while the proposed MIMO antenna is placed on the other side. The setup for the far-field measurements is shown in Fig. 8.

The simulated and measured radiation efficiency results of the proposed MIMO antenna are plotted in Fig. 9. The radiation efficiency is measured by exciting one port at a time and the rest of the ports are terminated with a 50Ω matched load. In figure 9, the radiation efficiency for 2.5 GHz frequency band (Ant-1 and Ant-2) is shown, and it is observed that the simulated radiation efficiency is greater than 95%, while the measured radiation efficiency varies in the range of 86-91%. For 3.5 GHz (Ant-5), shown in Fig. 9, the simulated radiation efficiency fluctuates in the range of 88-100%, while the measured radiation efficiency lies in the range of 87-92%.

The simulated and measured gain of the proposed MIMO antenna system for Ant-1, Ant-2, and Ant-5 is shown in

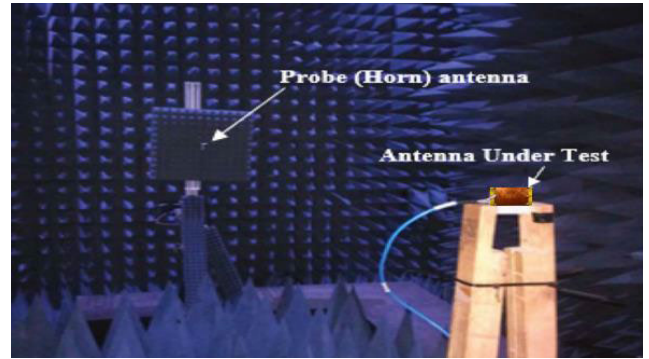


FIGURE 8. Far-field measurement setup.

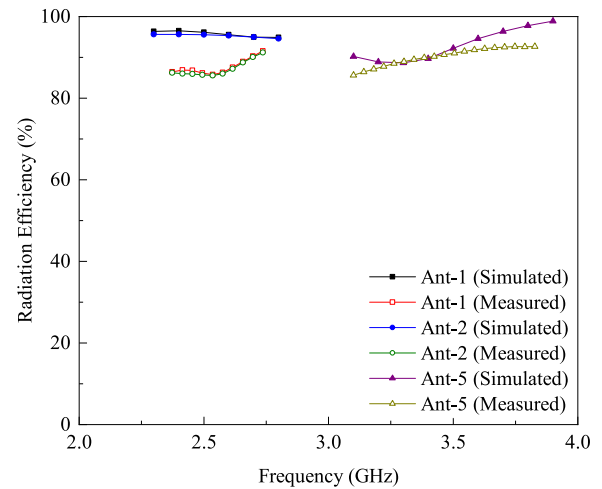


FIGURE 9. Simulated and measured radiation efficiency of the proposed MIMO antenna.

Fig. 10. For 2.5 GHz frequency band, shown in Fig. 10, the average simulated and measured gain values are > 4 dBi. On the other hand, the average simulated and measured gain for 3.5 GHz (see Fig. 10) fluctuates in the range of 4-6 dBi.

The simulated and measured radiation characteristics of the proposed MIMO antenna for Ant-1, Ant-2, Ant-5, and Ant-6 are shown in Fig. 11. To measure the radiation patterns in both the planes, two different measurements are carried out in an anechoic chamber where the proposed MIMO antenna is placed horizontally and vertically for $\phi = 0^\circ$ and 90° , respectively. It can be noted from the figure that Ant-1 and Ant-2 offer almost omnidirectional radiation characteristics for both planes. On the other hand, Ant-5 and Ant-6 provide typical monopole-like patterns in xz -plane ($\phi = 0^\circ$) and dual-beam properties in yz -plane ($\phi = 90^\circ$), which is also useful for short-range communication. One can also observe from Fig. 11 that the proposed MIMO antenna offers pattern diversity performance for both bands.

IV. MIMO PERFORMANCE PARAMETERS

To analyze the diversity of the proposed antenna system in MIMO channels, MIMO performance parameters, such

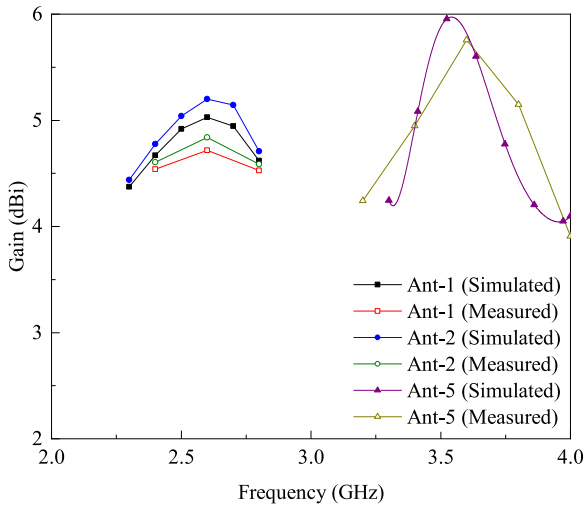


FIGURE 10. Simulated and measured gain of the proposed MIMO antenna.

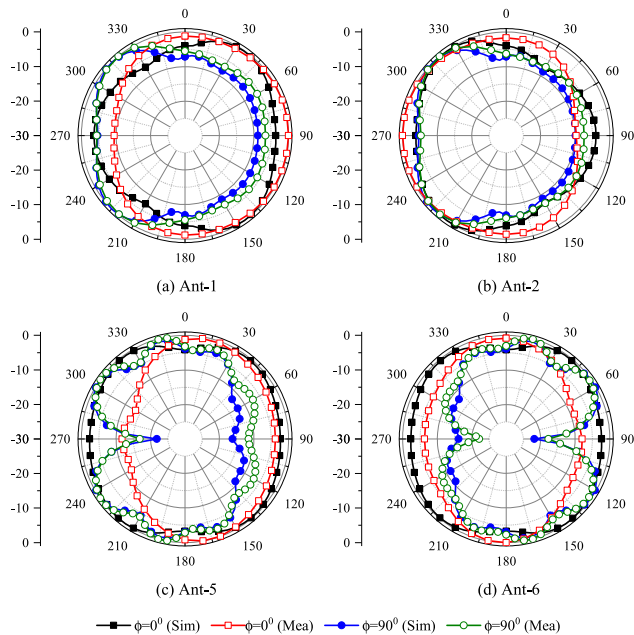


FIGURE 11. Simulated and measured radiation characteristics of the proposed MIMO antenna.

as ECC, TARC, and DG are evaluated in this section. The detail of such parameters along with the required results is presented in the following sections.

A. ENVELOP CORRELATION COEFFICIENT AND DIVERSITY GAIN

The ECC is one of the important factors to evaluate the performance of MIMO antennas. In an ideal scenario, the MIMO system requires an ECC equal to zero. Mathematically, ECC can be calculated by using the radiated fields of the MIMO

antenna system as [9]:

$$ECC = \frac{|\iint_{4\pi} (\vec{M}_i(\theta, \phi)) \times (\vec{M}_j(\theta, \phi)) d\Omega|^2}{\iint_{4\pi} |(\vec{M}_i(\theta, \phi))|^2 d\Omega \iint_{4\pi} |(\vec{M}_j(\theta, \phi))|^2 d\Omega} \quad (3)$$

where $\vec{M}_i(\theta, \phi)$ and $\vec{M}_j(\theta, \phi)$ represent the radiation patterns when antennas i and j are excited, respectively; and the term Ω denotes the solid angle.

For the proposed MIMO antenna configuration, the value of ECC for Ant_{1,2} and Ant_{5,6} at the desired frequency bands (2.5 GHz and 3.5 GHz) is less than 0.125 and 0.05 as shown in Fig. 12. Furthermore, for Ant_{1,5} and Ant_{2,5}, the observed value of ECC is less than 0.17 and 0.125 for 2.5 GHz and 3.5 GHz frequency bands, respectively. These results also indicate that the proposed MIMO system offers good isolation characteristics between antenna elements, which is an important factor for simultaneous operation.

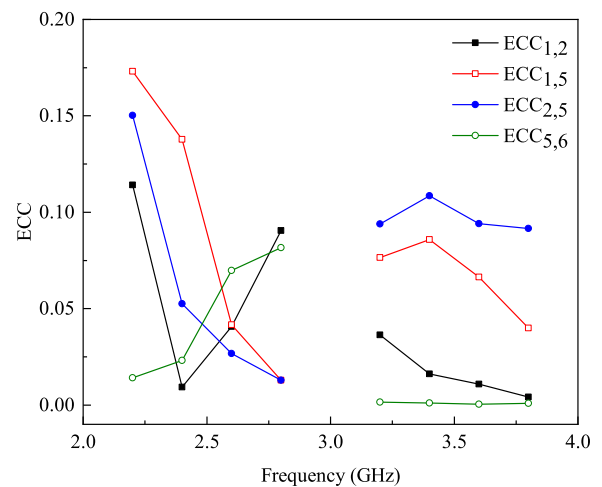


FIGURE 12. Envelop correlation coefficient of the proposed MIMO antenna.

On the other hand, the DG of the proposed MIMO antenna system can be calculated as [26]:

$$DG(dB) = 10 \log \left(\sqrt{1 - ECC^2} \right) \quad (4)$$

From Fig. 13, one can observe that the value of DG between Ant_{1,2} and Ant_{5,6} for 2.5 GHz frequency band is $geq 9.4$ dB and $geq 9.6$ dB, respectively; while for 3.5 GHz frequency band, it is >9.8 dB. Furthermore, for adjacent antenna elements (Ant_{1,5} and Ant_{2,5}), the value of DG is >9 dB for 2.5 GHz frequency band and >9.4 dB for 3.5 GHz frequency band.

B. TOTAL ACTIVE REFLECTION COEFFICIENT

The TARC is also considered to be an important parameter to assess the performance of the MIMO antenna system. It can be calculated as [27]:

$$TARC = \sqrt{\frac{(S_{mm} + S_{mn})^2 (S_{nm} + S_{nn})^2}{2}} \quad (5)$$

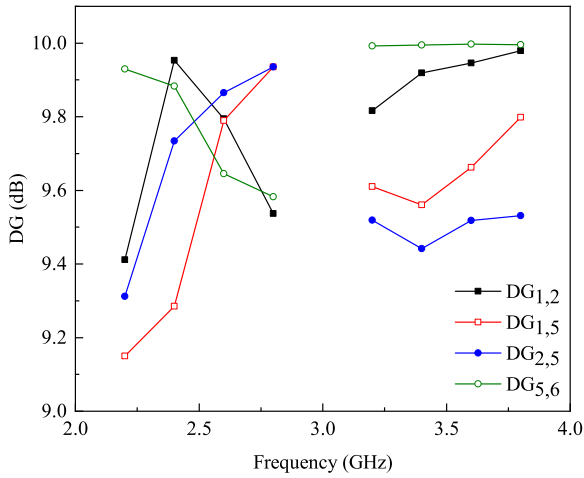


FIGURE 13. Diversity gain of the proposed MIMO antenna.

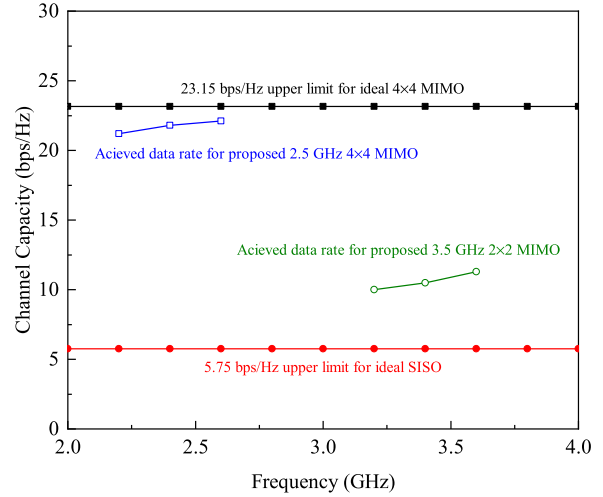


FIGURE 15. Ergodic channel capacity of the proposed MIMO antenna.

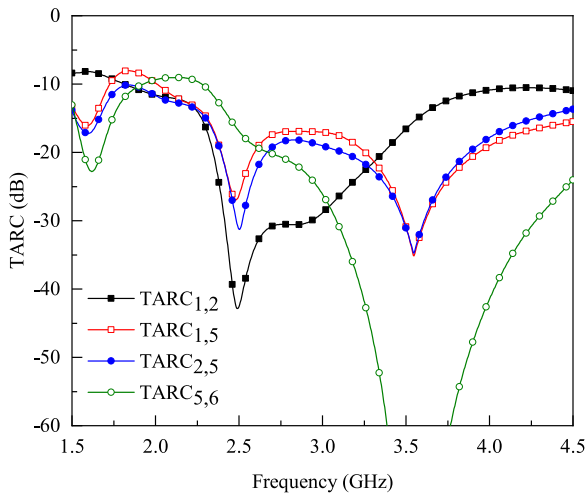


FIGURE 14. Total active reflection coefficient of the proposed MIMO antenna.

From the results, shown in Fig. 14, it is observed that the proposed MIMO antenna system provides TARC < -20 dB at 2.5 GHz and < -30 dB at 3.5 GHz. According to the obtained results, it can be concluded that the proposed design is highly suitable for MIMO applications.

C. ERGODIC CHANNEL CAPACITY

The ergodic channel capacity (CC) for the proposed MIMO antenna is calculated using the assumption used in [23], with the same amount of power provided to each transmit antenna and no prior knowledge of the channel state information (CSI) as calculated with the help of the following expression:

$$CC = E \left\{ \log_2 \left[\det \left(I + \frac{SNR}{m_{tr}} HH^T \right) \right] \right\} \quad (6)$$

where the channel matrix H can be computed as:

$$H = \sqrt{R_{TR}}G\sqrt{R_{Rre}} \quad (7)$$

The term E in (6) denotes the expectation concerning channel realization, I represent the identity matrix, SNR means signal to noise ratio at the receiver end, m_{tr} is the number of transmitting antennas, and $(.)^T$ represent the Hermitian transpose. Furthermore, it is assumed for this study that the transmitting antennas are uncorrelated with ($ECC = 0$) as represented by correlation matrix of R_{Tr} and receiver antenna correlation matrix given by R_{Rre} . The randomness of the channel is represented by matrix G that contains complex Gaussian random numbers. Hence, the channel matrix contains entries with dimensions of 4×4 matrix for 4-elements and 2×2 matrix for 2-elements. Hence, the ergodic CC is obtained by averaging over 10,000 independent and identical Rayleigh fading realizations with reference SNR of 20 dB [28]. The CC of the proposed MIMO antenna system for 2.5 GHz and 3.5 GHz is illustrated in Fig. 15. As can be observed from the figure that the calculated CC of the proposed design for 4×4 and 2×2 MIMO within the desired frequency bands is better than 20 bps/Hz and 10 bps/Hz, respectively; whereas for the ideal scenario, this value is equal to 23.15 bps/Hz [29].

V. IMPACT OF USER ON ANTENNA'S PERFORMANCE

This section describes the impact of the user on MIMO antenna performance. The performance is assessed in terms of reflection coefficient, radiation efficiency, and gain [30], [31]. Different usage postures such as the effects of single and double hands are investigated. According to the simulations, shown in Figs. 16 and 17, the designed MIMO antenna exhibits acceptable reflection coefficient and radiation characteristics in the vicinity of the human hand. It can be observed from Figs. 16(c) and 17(c) that the efficiency of the antenna elements has been decreased compared to Fig. 9. In a single-hand scenario, the maximum reduction in radiation efficiency has been observed for Ant-1, Ant-3, and Ant-6, while in a double-hand scenario, the reduction in radiation efficiency has been observed for Ant-2 and Ant-3.

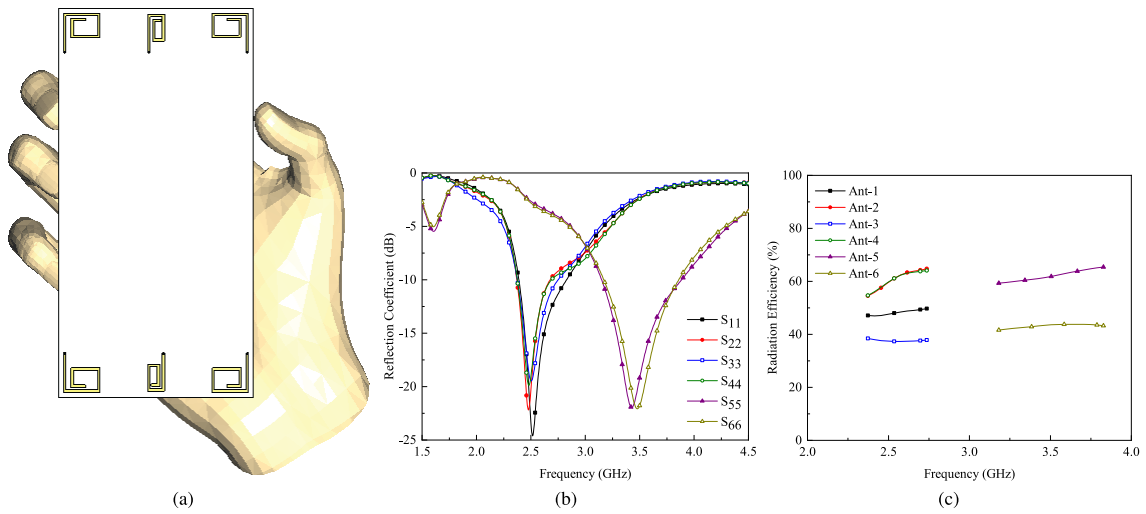


FIGURE 16. (a) Placement (b) reflection coefficient, and (c) radiation efficiencies of the proposed MIMO antenna in user's single hand.

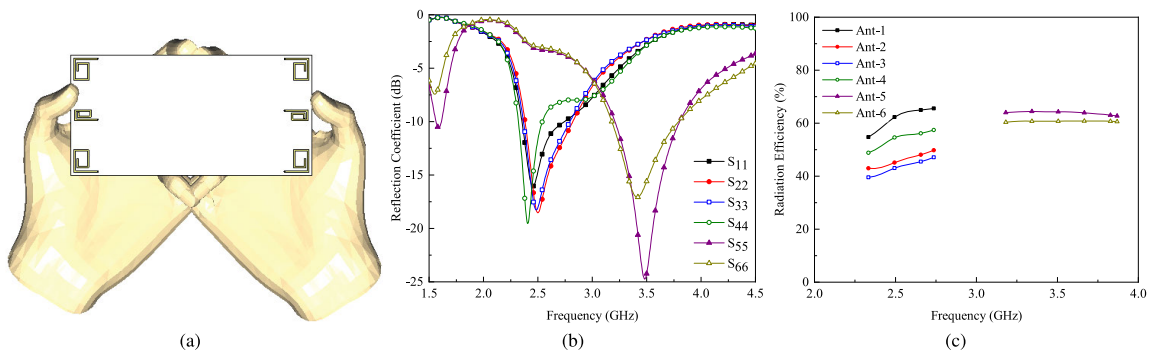


FIGURE 17. (a) Placement (b) reflection coefficient, and (c) radiation efficiencies of the proposed MIMO antenna in user's double hand.

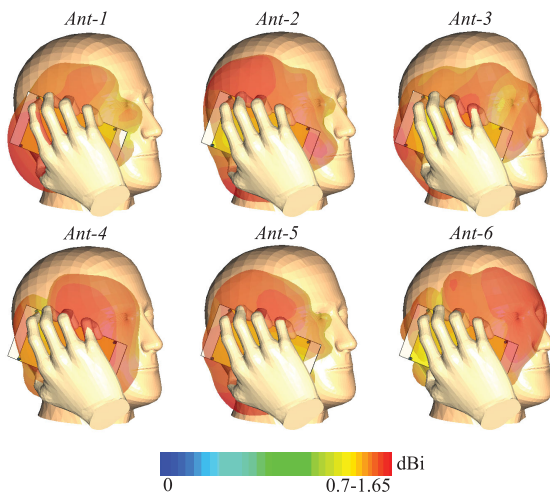


FIGURE 18. 3-D transparent radiation patterns of the proposed MIMO antenna in talk-mode scenario.

This reduction is due to the nature of body tissue properties, which can highly absorb an antenna radiation power. In general, the proposed MIMO antenna provides 40-70% radiation efficiencies for the operating bands.

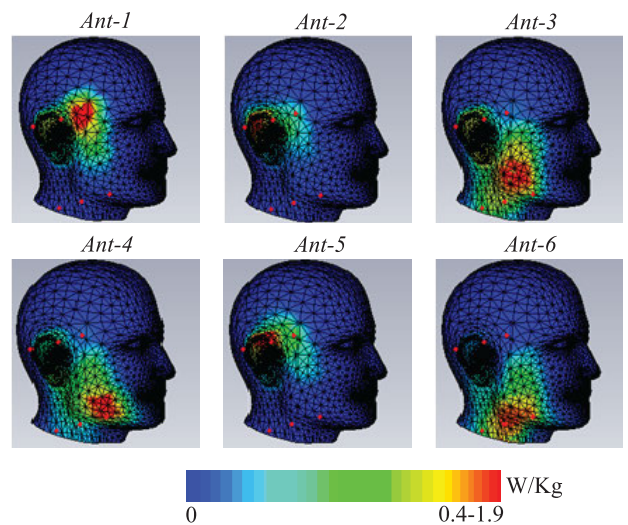


FIGURE 19. SAR analysis of the proposed MIMO antenna.

For talk-mode, the 3-D radiation patterns for each antenna element are shown in Fig. 18. From the figure, it has been demonstrated that the proposed design provides sufficient

radiation coverage with a gain level that varies from 0.7 to 1.15 dBi for 2.5 GHz frequency band, while it varies in the range of 1.14–1.65 dBi for 3.5 GHz frequency band.

One of the critical issues called specific absorption rate (SAR) also needs to be identified for antenna meant for mobile phone applications. The SAR measures the absorption level of electromagnetic waves in a human body [32]. For our proposed design, the SAR characteristic of our proposed MIMO antenna system with user-head are investigated and illustrated in Fig. 19. The maximum and minimum SAR for the proposed MIMO antenna is noted to be 1.9 W/Kg and 0.409 W/Kg, respectively; for Ant-2 and Ant-3. It can be concluded that the close distance between elements and the head phantom leads to a maximum SAR value and vice versa.

VI. CONCLUSION

A MIMO antenna design is presented for sub-6 GHz 5G mobile applications. The proposed design consists of six loop-type radiators designed at the corners and in the center of a smartphone board. The resonant frequency of the radiators placed at the edge is 2.5 GHz, which also follows the design configuration of pattern diversity, while the center placed radiators resonating at 3.5 GHz. Different MIMO antenna characteristics such as S-parameters, radiation efficiency, gain, radiation patterns, ECC, DG, and TARC are discussed in detail. Furthermore, to validate the simulation results, a prototype of the proposed MIMO antenna was fabricated and measured. In addition, the effect of a user on the antenna's performances is provided and it is observed that the proposed MIMO antenna offers acceptable characteristics in data mode as well as talk mode. Therefore, from the presented results, it can be concluded that the designed MIMO antenna provides sufficient features and fulfill the requirements of 5G-enabled mobile phones.

REFERENCES

- [1] Q.-U.-A. Nadeem, A. Kammoun, M. Debbah, and M.-S. Alouini, "Design of 5G full dimension massive MIMO systems," *IEEE Trans. Commun.*, vol. 66, no. 2, pp. 726–740, Feb. 2018.
- [2] A. Osseiran, F. Boccardi, V. Braun, K. Kusume, P. Marsch, M. Maternia, O. Queseth, M. Schellmann, H. Schotten, H. Taoka, H. Tullberg, M. A. Uusitalo, B. Timus, and M. Fallgren, "Scenarios for 5G mobile and wireless communications: The vision of the METIS project," *IEEE Commun. Mag.*, vol. 52, no. 5, pp. 26–35, May 2014.
- [3] H. H. Yang, *Massive MIMO Meets Small Cell*. Singapore: Springer, 2017.
- [4] R. Hussain, A. T. Alreshaid, S. K. Podilchak, and M. S. Sharawi, "Compact 4G MIMO antenna integrated with a 5G array for current and future mobile handsets," *IET Microw., Antennas Propag.*, vol. 11, no. 2, pp. 271–279, 2017.
- [5] N. O. Parchin, H. J. Basherlou, Y. Al-Yasir, R. Abd-Alhameed, A. Abdulkhaleq, and J. Noras, "Recent developments of reconfigurable antennas for current and future wireless communication systems," *Electronics*, vol. 8, no. 2, p. 128, Jan. 2019.
- [6] Q. Chen, H. Lin, J. Wang, L. Ge, Y. Li, and T. Pei, "Single ring slot-based antennas for metal-rimmed 4G/5G smartphones," *IEEE Trans. Antennas Propag.*, vol. 67, no. 3, pp. 1476–1487, Mar. 2019.
- [7] A. Zhao and Z. Ren, "Size reduction of self-isolated MIMO antenna system for 5G mobile phone applications," *IEEE Antennas Wireless Propag. Lett.*, vol. 18, no. 1, pp. 152–156, Jan. 2019.
- [8] L. B. Sun, H. Feng, Y. Li, and Z. Zhang, "Compact 5G MIMO mobile phone antennas with tightly arranged orthogonal-mode pairs," *IEEE Trans. Antennas Propag.*, vol. 66, no. 11, pp. 6364–6369, Nov. 2018.
- [9] M. Abdullah, S. H. Kiani, and A. Iqbal, "Eight element multiple-input multiple-output (MIMO) antenna for 5G mobile applications," *IEEE Access*, vol. 7, pp. 134488–134495, 2019.
- [10] Z. Ren, A. Zhao, and S. Wu, "MIMO antenna with compact decoupled antenna pairs for 5G mobile terminals," *IEEE Antennas Wireless Propag. Lett.*, vol. 18, no. 7, pp. 1367–1371, Jul. 2019.
- [11] W. Jiang, B. Liu, Y. Cui, and W. Hu, "High-isolation eight-element MIMO array for 5G smartphone applications," *IEEE Access*, vol. 7, pp. 34104–34112, 2019.
- [12] X. Zhang, Y. Li, W. Wang, and W. Shen, "Ultra-wideband 8-port MIMO antenna array for 5G metal-frame smartphones," *IEEE Access*, vol. 7, pp. 72273–72282, 2019.
- [13] S. H. Kiani, A. Altaf, M. Abdullah, F. Muhammad, N. Shoaib, M. R. Anjum, R. Damaševičius, and T. Blažauskas, "Eight element side edged framed MIMO antenna array for future 5G smart phones," *Micro-machines*, vol. 11, no. 11, p. 956, Oct. 2020.
- [14] H. Wang, R. Zhang, Y. Luo, and G. Yang, "Compact eight-element antenna array for triple-band MIMO operation in 5G mobile terminals," *IEEE Access*, vol. 8, pp. 19433–19449, 2020.
- [15] N. Kumar and R. Khanna, "A two element MIMO antenna for sub-6 GHz and mmWave 5G systems using characteristics mode analysis," *Microw. Opt. Technol. Lett.*, vol. 63, no. 2, pp. 587–595, Feb. 2021.
- [16] Y. Li, C.-Y.-D. Sim, Y. Luo, and G. Yang, "Multiband 10-antenna array for sub-6 GHz MIMO applications in 5-G smartphones," *IEEE Access*, vol. 6, pp. 28041–28053, 2018.
- [17] Y. Li, C.-Y.-D. Sim, Y. Luo, and G. Yang, "High-isolation 3.5 GHz eight-antenna MIMO array using balanced open-slot antenna element for 5G smartphones," *IEEE Trans. Antennas Propag.*, vol. 67, no. 6, pp. 3820–3830, Jun. 2019.
- [18] N. O. Parchin, H. J. Basherlou, M. Alibakhshikenari, Y. O. Parchin, Y. I. A. Al-Yasir, R. A. Abd-Alhameed, and E. Limiti, "Mobile-phone antenna array with diamond-ring slot elements for 5G massive MIMO systems," *Electronics*, vol. 8, no. 5, p. 521, May 2019.
- [19] N. O. Parchin, H. J. Basherlou, Y. I. A. Al-Yasir, A. M. Abdulkhaleq, M. Patwary, and R. A. Abd-Alhameed, "A new CPW-fed diversity antenna for MIMO 5G smartphones," *Electronics*, vol. 9, no. 2, p. 261, Feb. 2020.
- [20] N. O. Parchin, H. J. Basherlou, and R. A. Abd-Alhameed, "Design of multi-mode antenna array for use in next-generation mobile handsets," *Sensors*, vol. 20, no. 9, p. 2447, Apr. 2020.
- [21] N. O. Parchin, Y. I. A. Al-Yasir, H. J. Basherlou, R. A. Abd-Alhameed, and J. M. Noras, "Orthogonally dual-polarised MIMO antenna array with pattern diversity for use in 5G smartphones," *IET Microw., Antennas Propag.*, vol. 14, no. 6, pp. 457–467, May 2020.
- [22] R. Ullah, S. Ullah, R. Ullah, F. Faisal, I. B. Mabrouk, and M. J. A. Hasan, "A 10-ports MIMO antenna system for 5G smart-phone applications," *IEEE Access*, vol. 8, pp. 218477–218488, 2020.
- [23] R. Ullah, S. Ullah, F. Faisal, R. Ullah, I. B. Mabrouk, M. J. A. Hasan, and B. Kamal, "A novel multi-band and multi-generation (2G, 3G, 4G, and 5G) 9-elements MIMO antenna system for 5G smartphone applications," *Wireless Netw.*, vol. 27, pp. 4825–4837, Sep. 2021.
- [24] M. Zada, I. A. Shah, and H. Yoo, "Integration of sub-6-GHz and mm-wave bands with a large frequency ratio for future 5G MIMO applications," *IEEE Access*, vol. 9, pp. 11241–11251, 2021.
- [25] S. Islam, M. Zada, and H. Yoo, "Low-pass filter based integrated 5G smartphone antenna for sub-6-GHz and mm-wave bands," *IEEE Trans. Antennas Propag.*, vol. 69, no. 9, pp. 5424–5436, Sep. 2021.
- [26] A. Kumar, A. Q. Ansari, B. K. Kanaujia, and J. Kishor, "High isolation compact four-port MIMO antenna loaded with CSRR for multiband applications," *Frequenz*, vol. 72, nos. 9–10, pp. 415–427, Aug. 2018.
- [27] M. S. Sharawi, "Printed multi-band MIMO antenna systems and their performance metrics [wireless corner]," *IEEE Antennas Propag. Mag.*, vol. 55, no. 5, pp. 218–232, Oct. 2013.
- [28] M. Abdullah, S. H. Kiani, L. F. Abdulrazak, A. Iqbal, M. A. Bashir, S. Khan, and S. Kim, "High-performance multiple-input multiple-output antenna system for 5G mobile terminals," *Electronics*, vol. 8, no. 10, p. 1090, Sep. 2019.
- [29] Y. Li, H. Zou, M. Wang, M. Peng, and G. Yang, "Eight-element MIMO antenna array for 5G/sub-6 GHz indoor micro wireless access points," in *Proc. Int. Workshop Antenna Technol. (iWAT)*, Mar. 2018, pp. 1–4.
- [30] N. Ojaroudiparchin, M. Shen, and G. F. Pedersen, "Small-size tapered slot antenna (TSA) design for use in 5G phased array applications," *Appl. Comput. Electromagn. Soc. J.*, vol. 32, no. 3, pp. 193–202, 2017.

- [31] I. Syrytsin, S. Zhang, and G. F. Pedersen, "Performance investigation of a mobile terminal phased array with user effects at 3.5 GHz for LTE advanced," *IEEE Antennas Wireless Propag. Lett.*, vol. 16, pp. 1847–1850, 2016.
- [32] J. Moustafa, N. McEwan, R. Abd-Alhameed, and P. Excell, "Low SAR phased antenna array for mobile handsets," *Appl. Comput. Electromagn. Soc. J.*, vol. 21, no. 3, p. 196, 2006.



UZAIR AHMAD received the B.S. degree in telecommunication engineering from BUITEMS, Quetta, Pakistan. He is currently pursuing the M.S. degree in telecommunication engineering with the University of Engineering and Technology, Peshawar, Pakistan. He is also working as a Project Engineer at NRTC. His research interests include MIMO antenna design for future 5G mobile and base-station applications.



SADIQ ULLAH (Senior Member, IEEE) received the B.Sc. degree in electrical engineering from the University of Engineering and Technology, Peshawar, Pakistan, and the M.Sc. degree in electrical engineering from the University of Engineering and Technology Taxila, Pakistan. In 2007, he joined the Department of Electronic and Electrical Engineering, Loughborough University, U.K., and was awarded Ph.D. degree for his research in the field of design and measurement

of metamaterial-based antennas, in 2010. He worked as an Assistant Manager (Electronics) with a public sector Research and Development Organization, Islamabad, where his main responsibilities were hardware, software co-design, designing and testing of high precision electronics, test equipment. He has been worked as a Research Associate at Loughborough University, where he did research on the propagation effects of rain, snow, ice, fog, and forest in the millimeter-wave bands. He is currently a Professor and the Head of Telecommunication Engineering Department, University of Engineering & Technology, Mardan, Pakistan. His research is published in international conferences and peer-reviewed journals. His research interests include design and measurement of metasurfaces, metamaterial-based antennas, 5G MIMO antennas, multiband/wideband antenna, SAR, and wearable antennas.



UMAIR RAFIQUE (Student Member, IEEE) received the B.S. degree in electronic engineering from Mohammad Ali Jinnah University (MAJU), Karachi, Pakistan, in 2011, and the M.S. degree in electronic engineering from the Capital University of Science and Technology (CUST), Pakistan, in 2017. He is currently pursuing the Ph.D. degree in applied electromagnetics with the DIET Department, Sapienza Università di Roma, Rome, Italy. From 2010 to 2013, he worked with the Research

Group of Microelectronics and FPGAs at MAJU, as a Research Associate and a Research Fellow. In 2013, he joined AKSA Solutions Development Services (AKSA-SDS) as a RF Design Engineer, where he was responsible for the design and implementation of RF front-ends for airborne applications. In 2015, he joined the Research Group of Microelectronics and RF Engineering, CUST, as a Research Associate. He authored number of research articles in reputed international journals and conferences. His research interests include UWB antennas, MIMO antennas, near-field microwave imaging, metamaterials and metasurfaces, frequency selective surfaces, and semiconductor device modeling. He is a Registered Engineer from Pakistan Engineering Council (PEC).



the IEICE, JCN, KEES, IEEK, KICS, and ASK.

DONG-YOU CHOI received the B.S., M.S., and Ph.D. degrees from the Department of Electronics Engineering, Chosun University, Gwangju, South Korea, in 1999, 2001, and 2004, respectively. Since 2006, he has been a Professor and a Researcher with the Information and Communication Engineering Department, Chosun University. His research interests include rain attenuation, antenna design, wave propagation, and microwave and satellite communication. He is a member of



4G/5G wireless access points, and millimeter wave array antennas for 5G communication. His research is published in international conferences and peer-reviewed journals.

RIZWAN ULLAH was born in Khyber Pakhtunkhwa, Pakistan, in 1993. He received the B.Sc. and M.S. degrees in telecommunication engineering from the University of Engineering and Technology Peshawar, Pakistan, in 2016 and 2020, respectively. He is currently pursuing the Ph.D. degree in telecommunication engineering with UET, Mardan, Pakistan. His research interests include design and analysis MIMO antennas for 4G and 5G smartphone, MIMO antennas for



BABAR KAMAL received the bachelor's degree from BUITEMS, Quetta, in 2012, and the master's degree from the Telecommunication Engineering Department, UET, Peshawar, in 2016. He is currently pursuing the Ph.D. degree with the School of Marine Science and Technology, NWPU, China. His research interests include metasurfaces, metamaterials, wearable antennas, multiband/wideband antennas, polarization control devices, and absorbers.



spheric absorption rate analysis, and EBGs.

ASHFAQ AHMAD received the bachelor's degree in telecommunication engineering from UET Peshawar, in 2016, and the master's degree in telecommunication engineering from UET Taxila, in 2018. He is currently a Research Associate with the Department of Information and Communication Engineering, Chosun University, Gwangju, South Korea. His research interests include planar antenna, millimeter wave antennas, MIMO antennas, multi band antennas, implanted antennas, specific

...